

# Characterization of two biodegradable polymers of potential application within the biomaterials field

R. L. REIS\*

*Department of Metallurgical Engineering, FEUP, University of Porto, Rua dos Bragas, 4099 Porto Codex, Portugal and INEB - Institute for Biomedical Engineering, Praça do Coronel Pacheco 1, 4050 Porto, Portugal*

A. M. CUNHA

*DEP - Department of Polymer Engineering, University of Minho, Campus de Azurém, 4800 Guimarães, Portugal*

---

An extensive characterization of two biodegradable polymers that may constitute an alternative, if one is aiming at orthopaedic applications, to the currently used poly(glicolic acid), poly(lactic acid) or polyhydroxybutyrate was carried out. A cellulose acetate and three different grades of a novel starch based polymer were studied. The characterization included: tensile and instrumented impact tests, rheological measurements, scanning electron microscopy (SEM), X-ray diffraction (XRD), Fourier transformed infra-red spectroscopy (FTIR), differential scanning calorimetry (DSC), and long-term degradation trials in Hank's solution. The results show that both polymers, specially the starch based one, present a great potential for biomedical applications, on which adequate mechanical properties associated to a controlled degradation rate are required.

---

## 1. Introduction

Biodegradable polymers are very useful in the biomaterials field. Their use in medical devices is becoming more commonplace every day [1–4]. Examples of reported applications include surgical sutures and implants, drug carriers and drug delivery systems [4]. However, the number of polymers in clinical use is still rather small, and further research is required to introduce new materials, allowing for new applications and devices to emerge.

Currently available biodegradable polymers include polyglycolic acid (PGA) [5], polylactic acid (PLA) [5–6], polyhydroxybutyrate (PHB) [1, 7]. Special research efforts are focusing on the development of biodegradable polymers for fracture fixation [8–10]. Materials to be used in these applications must compromise adequate mechanical properties with controlled degradability by human fluids [5, 9–10]. Metallic implants have been used for bone fracture fixation for many years. However, the load sharing between the device and bone is in proportion to their relative stiffness. The complete healing of the bone requires a certain degree of mechanical solicitation, being, therefore, prevented as long as the device is present and bears most of the load [8–10]. Also, the early removal of the fixation plate can leave the bone temporarily weak and subject to refracture. The

replacement of a metallic fracture fixation device with a bioabsorbable polymer or composite, that has an appropriate combination of initial strength and stiffness, may be very advantageous: i) the expectable reduction in the modulus of the material should lead to a gradual load transfer to the healing bone; and ii) eventually the complete absorption of the implant may avoid a second operation to its removal.

In fact, this study presents, as a preliminary report, an extensive characterization of two materials, a cellulose acetate (CA) and a starch/poly(ethylene-vinyl alcohol) copolymer (SEVA), aiming at orthopaedic applications. In fact cellulose and starch based polymers are two well known biodegradable polymers [11–14], exhibiting a great potential, for being an alternative to the more usual PLA, PGA and PHB. Nevertheless, their biomedical possible uses are not fully investigated.

## 2. Materials and methods

Two different polymers were selected for this study: —a cellulose acetate—Dexel, from Courtaulds Plastics, UK, with a melt flow index (MFI) of 3.67 g/600 s (200 °C, 21 N);—three grades of a 60/40 (mol/mol) starch/poly (ethylene-vinyl alcohol) copolymer—Mater-Bi from Novamont, Italy, with a MFI (170 °C,

\*To whom correspondence should be addressed.

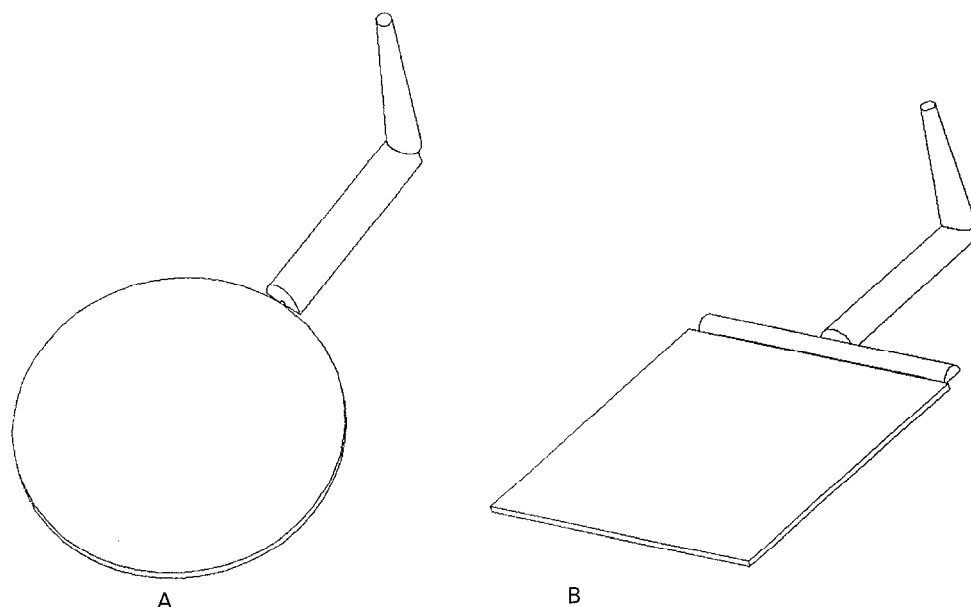


Figure 1 Schematic drawing of the mouldings: A—pin gated circular plate, B—film gated square plate.

TABLE I Relevant processing parameters for SEVA and CA

Material	$T_{inj}$ (°C)	$T_{mould}$ (°C)	Flow rate (cm <sup>3</sup> /s)	$P_{hold}$ (MPa)	Cycle time (s)
SEVA	170	60	40	70	35
CA	200	40	30	50	40

$T_{inj}$ -injection temperature;  $T_{mould}$ -mould temperature;  $P_{hold}$ -holding pressure

49 N) of respectively 19.28 g/600 s (grade A, trade name Mater-Bi SAO31), 2.64 g/600 s (grade B, trade name Mater-Bi AIO5H) and 0.71 g/600 s (grade C, trade name Mater-Bi 1128RR).

The materials were injection moulded on a Krauss Maffei KM-60/120A machine at 200 °C for CA and 170 °C for SEVA, in order to produce standard ISO tensile samples and impact plates 2 mm thick with two different geometries (round-60 mm diameter and square-60 mm size). Fig. 1 presents a schematic drawing of the plates and respective runner systems. The processing conditions are presented in more detail on Table I.

The characterization of the materials included several experimental techniques, namely:

- tensile testing in an Instron 4505;
- rheological studies in a Rosand capillary rheometer;
- scanning electron microscopy (SEM) in a Leica Cambridge instrument;
- Fourier transformed infra-red spectroscopy (FTIR) in a Perkin Elmer 1600 Series;
- X-ray diffraction (XRD) in a Philips equipment with a PW1710 control unit,
- differential scanning calorimetry (DSC) in Perkin-Elmer Series 7 thermal analysis system;
- instrumented impact in a falling weight Rosand Tester type 5;
- long-term degradation tests in Hank's solution.

The tensile tests were carried out in order to determine the modulus ( $E$ , at  $\epsilon = 1\%$ ), ultimate tensile strength (UTS) and elongation at break ( $\epsilon_r$ ). The secant modulus was determined with a resistive extensometer. All tests were carried out at room temperature ( $20 \pm 2$  °C) at a crosshead speed of 50 mm/min ( $8.3 \times 10^{-4}$  m/s), using ISO standard tensile samples.

Rheological studies were performed for the three different grades of SEVA at 170 °C (processing temperature) and 150 °C. These tests were done using a double die geometry system,  $l = 16$  mm/ $\phi = 1$  mm (long die) and  $l = 0.2$  mm/ $\phi = 1$  mm (short die), with a constant entry angle of 180°. The applied shear stresses were controlled by means of programming the piston velocity. Rabinowitsch and Bagley corrections were used in all calculations.

SEM examination was planned to enable a morphological evaluation of the fracture surfaces originated by tensile and impact experiments and to observe the changes induced by degradation trials. All samples were coated with a thin film of gold, prior to any observation, by ion sputtering. The electron beam energy was always 25 KeV. Both secondary and backscattered electron images were obtained and registered in photographic film.

The utilization of FTIR was selected in order to assess possible changes on the chemical structure of the polymers, that might have been induced by the processing routes or the long-term degradation tests. It has been reported [12] that starch based polymers are very sensitive to thermal degradation during processing, specifically when high residence times are involved. The samples were prepared in the form of very thin films by a hot compression technique. IR data manager software, associated to the Perkin Elmer 1600 series FTIR equipment, was utilized for analysing the obtained spectra.

X-ray diffraction studies were conducted using wide angle type conditions. Spectra were obtained at

a scanning rate of 0.02°/min, using copper  $K_{\alpha}$  radiation ( $\lambda = 1.5418 \text{ \AA}$ ), with a nickel filter (without any monochromator). The  $2\theta$  angles were scanned from 6 to 60°, with the power generator at 36 kV, 26 mA. For data acquisition purposes and data treatment a SIE R.Y 112 software from SIETRONIC was used. The crystallinity of the samples was estimated by weighting the relative area of the peaks and of the amorphous background.

DSC thermograms were obtained after running three consecutive scans: i) 25 °C–170 °C (20 °C/min)–25 °C (500 °C/min), ii) 25 °C–170 °C: (20 °C/min)–25 °C (20 °C/min), iii) 25 °C–170 °C (20 °C/min). The first two runs were aimed at eliminating the samples previous thermal history. The samples, within a weight range from 5 to 7 mg (micro balance measurements), were introduced in standard aluminium capsules before starting the tests. This technique was used to compare the thermal behaviour of the three grades of SEVA, being obtained figures for the peak and melting temperatures and the melting enthalpy.

Impact tests were performed using a mass of 25 kg and a testing velocity of 1 m/s. Samples were both circular plates (pin gated) and square plates (film gated) with the dimensions already referred to. They were tested at three different temperatures: –10 °C, 23 °C (room temperature) and 37 °C (body temperature). The samples were peripherally clamped and supported by a cylindrical rig with an internal diameter of 40 mm. The peak energy ( $E_p$ ) and force ( $F_p$ ) and the total failure energy ( $E_f$ ) were computed (using a digital filter of 3 kHz) and analysed. A NAC high speed video unit (HSV) was used to follow the impact fracture evolution at times as small as  $10^{-3}$  s.

The long term degradation tests were carried out in a Hank's balanced salt solution Gibco 041-04025 M w/o phenol red (HBSS, composition: NaCl–8.0, CaCl<sub>2</sub>–0.14, KCl–0.40, NaHCO<sub>3</sub>–0.35, MgCl<sub>2</sub>·6H<sub>2</sub>O–0.10, Na<sub>2</sub>HPO<sub>4</sub>·2H<sub>2</sub>O–0.06, KH<sub>2</sub>PO<sub>4</sub>–0.06, MgSO<sub>4</sub>·7H<sub>2</sub>O–0.06, glucose–1.0 g/cm<sup>3</sup>) obtained from Life Technologies, Paisley, Scotland, UK. Samples were immersed at 37 °C  $\pm$  1 °C, in individual containers (volume of approximately 200 cm<sup>3</sup>) placed in a thermostatic immersion circulator, for times as long as 6 months and weighed on a regular basis in a precision balance. Before each weighing, samples were dried for 1 h at 60 °C. The percentage weight loss was calculated and plotted against time.

### 3. Results and discussion

The mechanical properties determined for both the cellulose acetate and the starch based grades are presented in Table II. Typical stress versus strain curves for the SEVA polymers are presented in Fig. 2. A wide range of mechanical behaviours was observed, from the brittleness of the higher molecular weight material, grade (C), to the ductile grade (A).

As the starch based material, according to XRD data (Fig. 3), proved to be around 50% crystalline, a processing route to induce anisotropy is being tested and it may allow an increase in the values of the tensile properties. Preliminary results, obtained using

TABLE II Tensile tests results for SEVA and CA materials

Material	UTS (MPa)	$E$ (GPa)	$\epsilon_r$ (%)	Energy to break (J)
SEVA-A	10.5	0.84	25.6	4.42
SEVA-B	23.1	1.20	6.0	3.24
SEVA-C	35.6	1.81	5.3	3.02
CA	26.5	1.58	21.7	10.47

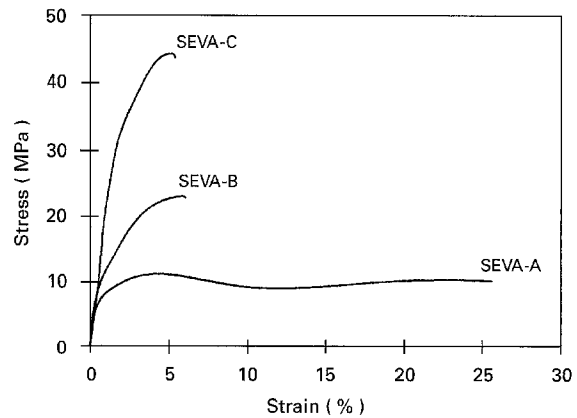


Figure 2 Stress versus strain plot for SEVA polymers as obtained in the tensile tests.

SCORIM technology (Shear Controlled Orientation in Injection Moulding) [15], ranged from 2.3 up to 3 GPa for the modulus, 35 to 42 MPa for UTS and 48 to 7% for  $\epsilon_r$ . Further details on this processing technology and on the attained mechanical properties may be found elsewhere [16], but it must be stressed that it was possible to obtain a higher stiffness and strength, associated with a much higher ductility. So, it is expected that processing optimization should be a route to achieve properties as those reported for the self-reinforced PLA [5–6], i.e close to those of bone. Also the reinforcement of the SEVA with bioactive materials, such as hydroxylapatite and bioactive glasses, is being assessed as has been previously reported for PLA materials [17]. The same approach used for UHMWPE/HA composites is being tested [18], in order to optimize mechanical performance throughout processing.

SEVA presents a much more brittle fracture than CA, both in tensile testing ( $8.3 \times 10^{-4}$  m/s) and under impact loading conditions (1 m/s). The distinct behaviour of the two materials, evidenced by the results in Tables II (tensile) and III (impact), was confirmed by HSV and SEM analysis of the fracture surfaces. Fig. 4 shows the typical fracture surfaces, featuring a brittle pattern of SEVA-C (with a clear nucleation point around a void) and a very ductile highly deformed morphology of CA.

The impact results pointed out clearly the differences between the materials analysed and their sensitivity to the test temperature and gate geometry of the mouldings. Pin gated samples of SEVA present a lower impact resistance as a result of the more violent thermo-mechanical conditions imposed on the polymer during processing. The opposite behaviour is shown by CA mouldings evidencing that this polymer

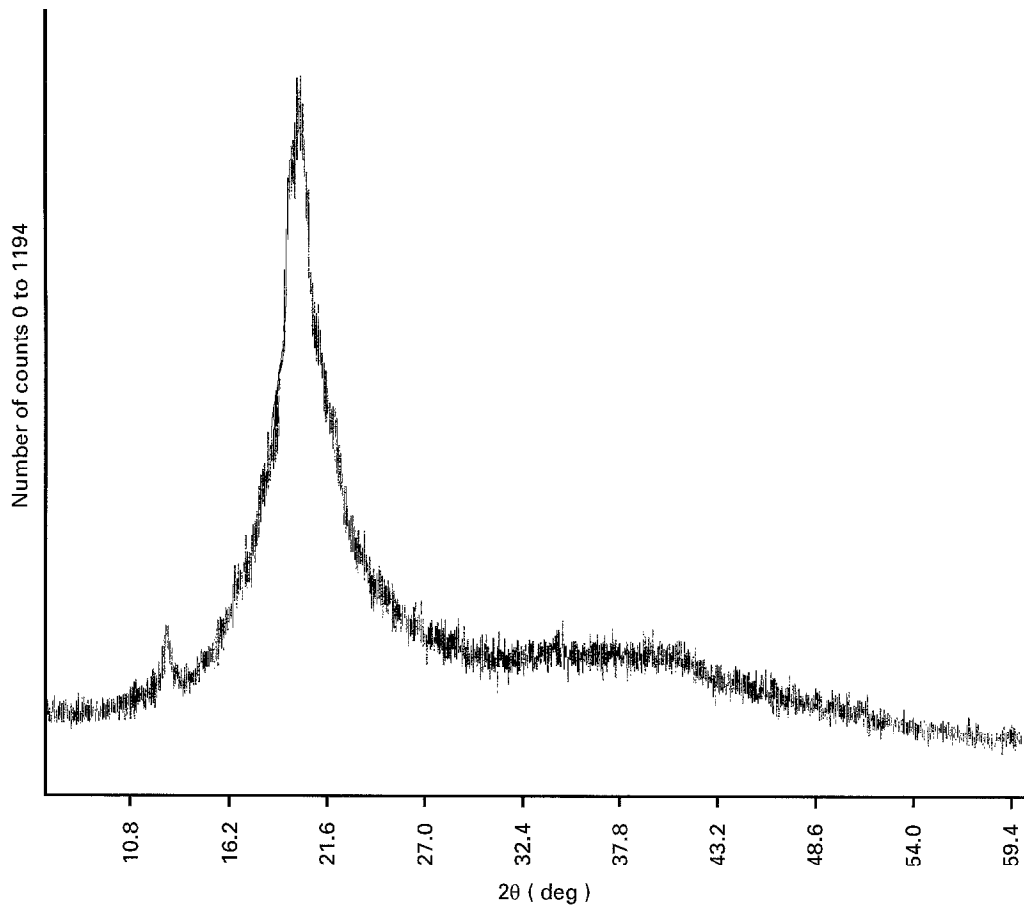


Figure 3 XRD pattern for SEVA-C. Peaks detected do not match any standard JCPDS file. Based on these patterns a crystallinity value of 45–50% was estimated for SEVA grades.

TABLE III Instrumented impact results for the two different gate types (pin and film), at  $-10^{\circ}\text{C}$ ,  $23^{\circ}\text{C}$  and  $37^{\circ}\text{C}$

Material	Testing temperature ( $^{\circ}\text{C}$ )	Gate type (Pin/Film)	Peak force, $F_p$ (N)	Peak energy, $E_p$ (J)	Fracture energy $E_f$ (J)
SEVA-A*	23	Pin	156.0	0.1440	0.7802
SEVA-A*	23	Film	203.2	0.1781	1.0202
SEVA-B	-10	Pin	189.5	0.0680	0.5425
	23		199.1	0.1197	0.5583
	37		203.7	0.1226	0.6667
SEVA-B	-10	Film	365.1	0.2107	0.6446
	23		363.6	0.2838	0.8224
	37		479.7	0.7076	0.9508
SEVA-C	-10	Pin	180.4	0.0584	0.4318
	23		195.0	0.0829	0.5836
	37		157.7	0.0704	0.4437
SEVA-C	-10	Film	262.7	0.1237	0.5540
	23		289.2	0.1726	0.7311
	37		240.5	0.1529	0.6276
CA	-10	Pin	959.6	1.8020	2.2495
	23		1508.8	3.8500	3.9413
	37		1302.0	3.7785	4.1315
CA	-10	Film	219.4	0.1138	0.4220
	23		923.0	1.7553	1.8003
	37		972.3	2.5367	2.8362

\*SEVA-A was only tested at room temperature

withstands well the very high stress field associated with the thin section of the pin gate. The unexpected decrease of impact performance of SEVA-C at  $37^{\circ}\text{C}$  should be associated to a modification of the samples moisture content caused by the heat aging before testing (48 h at  $37^{\circ}\text{C}$ ).

Fig. 5 presents a fracture evolution sequence for SEVA-C, while tested at  $37^{\circ}\text{C}$ . It may be observed that fracture initiation takes place in less than 1 ms, the propagation stage is based on the development of a star shape multi-fracture mechanism, and the complete failure of the sample occurs within 3 ms. The

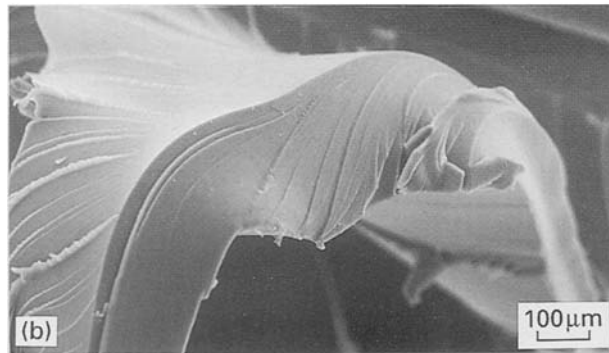
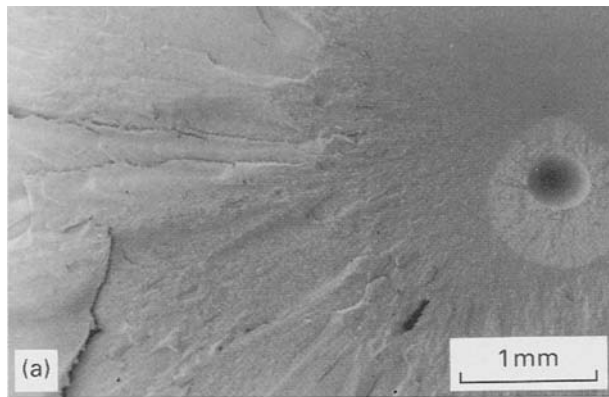


Figure 4 SEM photomicrographs of tensile fracture surfaces: A—SEVA-C (a well marked nucleation point is noticeable around a void), B—CA (presenting a very ductile behaviour).

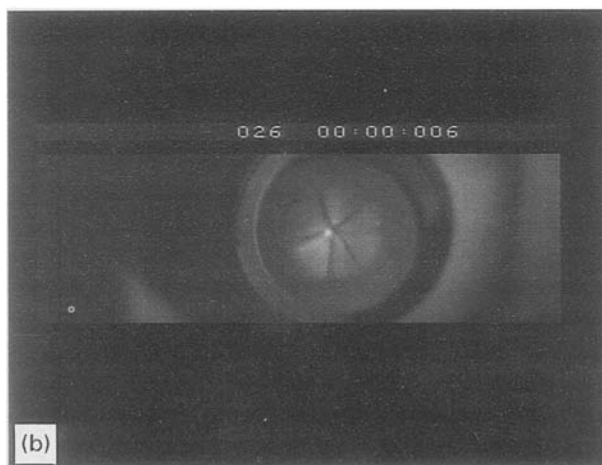
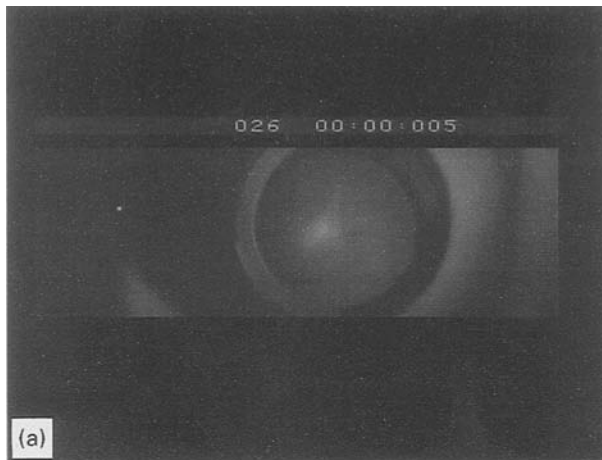


Figure 5 A sequence of the fracture evolution, during impact tests, as function of time. Pictures for 1 ms (A), 2 ms (B) and 3 ms (C) are presented. Fracture initiation occurs within the first millisecond.

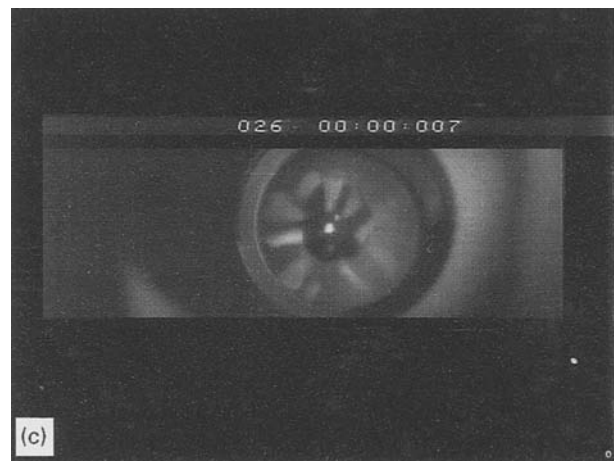


Figure 5 (Continued)

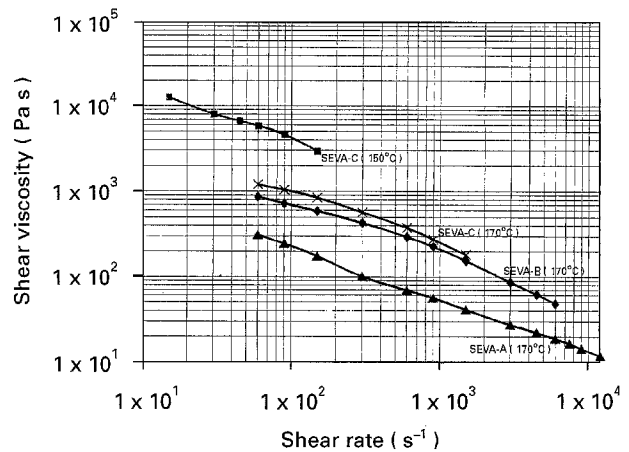


Figure 6 Flow curves for SEVA polymers.

characterization of the impact behaviour is not common in biomaterials, however it is very important when orthopaedic applications are concerned. Rheological behaviour of SEVA follows an expected dependence on both the material grade and the testing temperature (Fig. 6) and exhibits a shear thinning behaviour.

The DSC analysis (typical thermogram in Fig. 7) pointed out well defined crystalline peaks for the three SEVA grades, which confirms the XRD estimations previously discussed. Furthermore, both melting and peak temperatures (Table IV) increase with the molecular weight of the polymer (qualitatively estimated from MFI measurements). The melting enthalpies obtained indicate a non-negligible variation of the crystallinity between the three grades. However, this evidence was not detected by the XRD experiments.

Immersion studies at 37°C in Hank's solution provides evidence of the *in vitro* biodegradability of the two polymers studied. Fig. 8 shows degradation curves (percentage weight loss against time) for CA and SEVA grades. The extent of the degradation in the starch based polymers is highly dependent on the respective shear viscosity. For grade (A), the weight loss is more important and faster, without attaining a plateau during the testing period. As environmental stress cracking polymer degradation is well known,

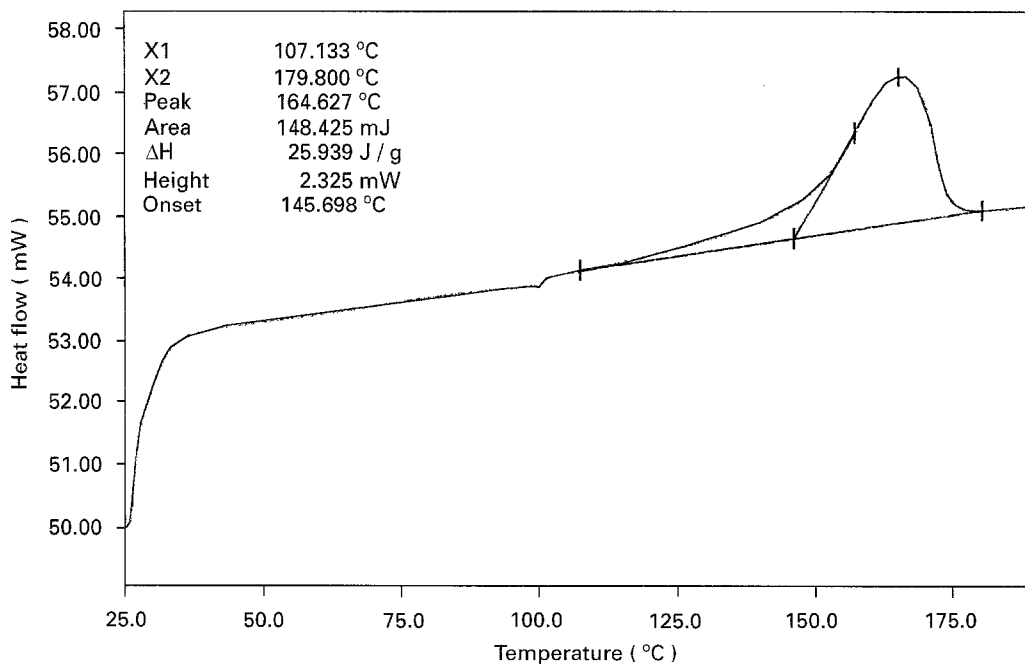


Figure 7 A typical DSC thermogram for SEVA-C. The semi-crystalline behaviour of the starch based polymer, it is clear.

TABLE IV DSC results for SEVA grades (Melt flow index values are also presented for all the grades)

Material	Melting temperature (°C)	Peak temperature (°C)	Melting enthalpy (J/g)	Melt flow index (g/600s)
SEVA-A	137.58	148.75	19.52	19.28
SEVA-B	141.37	158.27	24.64	2.64
SEVA-C	145.70	164.63	25.94	0.71

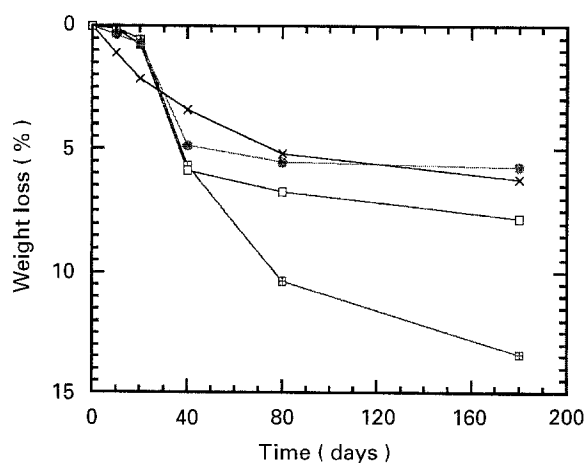
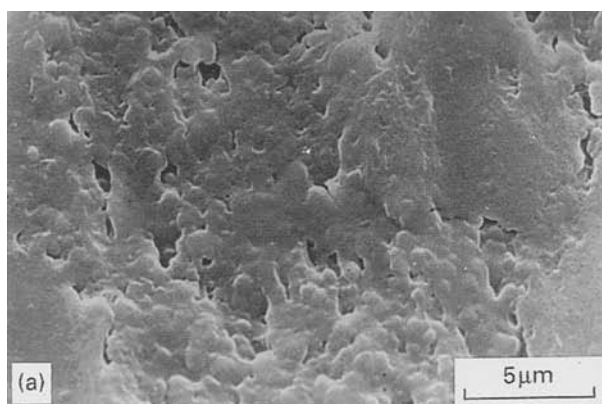


Figure 8 Weight loss (dry weight) versus time for SEVA grades and CA when immersed in HBSS at 37 °C. (□), SEVA-A; (○), SEVA-B; (●), SEVA-C; (×), CA.



experiments under load should be carried out in the future.

Fig. 9 shows two SEM photomicrographs of SEVA-C material surface, before and after 6 months degradation in HBSS. It is interesting to notice that the degraded sample shows a smooth surface compared to the very rough injection moulded one. This phenomenon should be related to a hydrolytic surface dissolution of the original sample.

Fig. 10 presents two FTIR spectra of SEVA-C, for the virgin raw material and pin gated injection moulded samples. The two spectra are qualitatively identical. This matching allows the conclusion that degradation during processing corresponds mainly to macromolecular breakage without important chemical changes in the polymer structure.

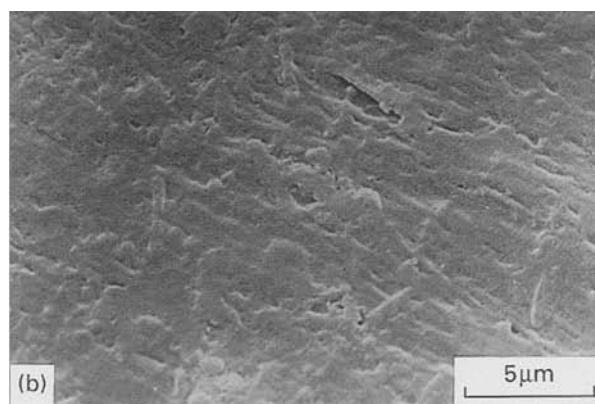


Figure 9 SEM photomicrograph of a SEVA-C surface. A—after moulding, B—after six months degradation in HBSS at 37 °C.

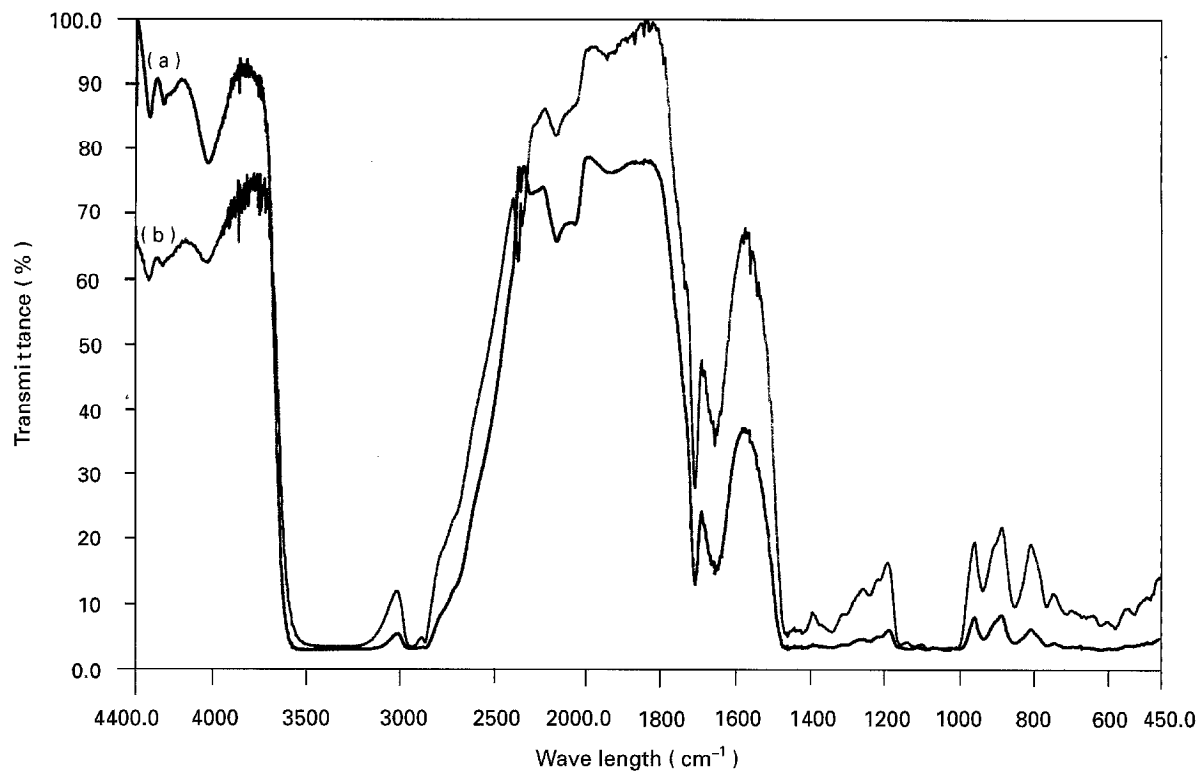


Figure 10 FTIR spectra for SEVA-C. A—virgin polymer, B—pin gated injection moulded sample. No sensible changes were detected.

#### 4. Conclusions

A preliminary extensive characterization of CA and SEVA indicated that these polymers have great potential for application as biomaterials. Nevertheless, further developments should be supported by a better knowledge of: i) the degradation mechanisms, and their effect on the performance of the materials and ii) the possibilities of improving mechanical properties (through processing and/or reinforcement).

#### Acknowledgements

The help of our colleagues from the Dept of Polymer Engineering/U. Minho, namely Paulo O. Leite, Ana V. Machado and Julio Viana was essential for carrying out this work. Also the technicians Mrs Fátima Machado from the SEM Lab. and Mr F. Mateus from the Polymer Processing Lab. are gratefully acknowledged. We would also thank the collaboration of Prof. M. J. Bevis and Dr P. Allan from Brunel University, London UK on the anisotropic processing of SEVA and Programme PRAXIS XXI for supporting Rui L. Reis.

#### References

1. J. C. KNOWLES and G. W. HASTINGS, *J. Mater. Sci.: Mater. in Medicine* **3** (1992) 352.
2. R. S. LANGER and N. A. PEPPAS, *Biomaterials* **2** (1981) 201.

3. I. CAPPERAULD, *Clin. Mater.* **4** (1989) 3.
4. T. HAYASHI, *Prog. Polym. Sci.* **19** (1994) 663.
5. P. TORMALA, *Clin. Mater.* **13** (1993) 35.
6. K. P. ANDRIANO, T. POHJONEN and P. TORMALA, *J. Apl. Biomater.* **5** (1994) 133.
7. J. C. KNOWLES and G. W. HASTINGS, *J. Mater. Sci.: Mater. in Medicine* **4** (1993) 102.
8. P. U. ROKKANEN, *Ann. Med.* **23** (1991) 109.
9. A. U. DANNIELS, K. P. ANDRIANO, W. P. SMUTZ, M. K. O. CHANG and J. HELLER, *J. Apl. Biomater.* **5** (1994) 51.
10. T. TERJESSEN and K. APALEST, *J. Orthop. Res.* **6** (1988) 293.
11. J. POUTIS, C. BAQUEY and D. CHAUVEAUX, *Clin. Mater.* **16** (1994) 119.
12. C. BASTIOLI, V. BELLOTTI, L. DEL GIUDICE and G. GILLI, *J. Environm. Polym. Degr.* **1** (1993) 181.
13. Y. H. LEE and L. T. FAN, *Biotechnol. Bioeng.* **24** (1982) 2383.
14. J. J. CAEL and J. L. KOENING, *Biopolymers* **14** (1975) 1885.
15. P. S. ALLAN and M. J. BEVIS, *Composites Manufacturing* **2** (1990) 79.
16. R. L. REIS, A. M. CUNHA, P. S. ALLAN and M. J. BEVIS, *J. Polym. for Advanc. Techn.* (submitted).
17. C. C. P. M. VERHEYEN, J. R. WIJN, C. A. VAN BLITTER-SWIJK and K. DE GROOT, *J. Biomed. Mater. Res.* **26** (1992) 1277.
18. A. M. CUNHA, R. L. REIS, F. FERREIRA and P. L. GRANJA, in "Advances in Materials Science and Orthopaedic Surgery, NATO/ASI Series E: Applied Sciences", edited by R. KOSSOWSKY, N. KOSSOWSKY, (Kluwer Press, Amsterdam, 1995) 163.

Received 29 June  
and accepted 4 July 1995